Polyoxometalate Intercalated Layered Double Hydroxides as Efficient and Recyclable Bi-functional Catalysts for Cascade Reactions

Kai Liu,[a†] Yanqi Xu,[a†] Zhixiao Yao,[a] Haralampos N. Miras[b*] and Yu-Fei Song [a*]

[a]State Key Laboratory of Chemical Resource Engineering, Beijing University of Chemical Technology, Beijing 100029, P. R. China. Tel/Fax: + 86 10 64431832; E-mail: songyufei@hotmail.com

[b]Department of Chemistry, University of Glasgow, Glasgow, G12 8QQ, UK. Tel: 0044 (0) 141 330 4375; Email: harism@chem.gla.ac.uk

† they have the same contribution

Abstracts: The polyoxometalate (POM) intercalated-layered double hydroxides (LDHs) have been widely used as heterogeneous catalysts. However, the application of POM-LDHs as bi-functional catalysts for cascade reaction has seldom been studied comparing with the noble metal-based catalysts. Herein, a series of POM-LDHs catalysts of Tris-LDH-$X_4(PW_9)_2$ (X = Mn, Fe, Co, Ni, Cu and Zn) has been prepared; The efficacy of Tris-LDH-$Zn_4(PW_9)_2$ as efficient bi-functional catalyst has been demonstrated for cascade reactions involving oxidation of benzyl alcohol to benzaldehyde followed by Knoevenagel condensation with ethyl cyanoacetate to produce benzylidene ethyl cyanoacetate. The combination of POM's redox/acidic sites and LDHs's basic sites led to a composite catalyst with excellent activity (99%) and selectivity ($\geq$ 99%) under mild and soluble-base-free conditions. This work offer a new design strategy for the fabrication of efficient bi-functional catalysts for the promotion of one-pot cascade reactions.

Introduction

One-pot cascade reactions have attracted the interest of organic synthetic chemists in recent years,[1-4] as they can dramatically simplify complex synthetic pathways, reduce the production wastes and energy consumption.[5-9] A feasible route for the efficient progression of cascade reactions, is based on the design of new catalysts with spatially isolated multiple active sites, which can promote simultaneously different reactions. To date, a wide variety of catalytic systems have been proposed for cascade reactions, however many of these are based on homogeneous catalysts.[10,11] In contrast to homogeneous catalysts, their heterogeneous counterparts exhibit significant advantages such as facile recovery and recyclability, least possible contamination of the reaction medium as well as high stability. Although the catalytic efficacy of heterogeneous catalysts such as Au/TiO_2,[12] Au–Pd/resin[13], Pd/MOF[14] and Pt/polymer[15] *etc.* in cascade reactions has been demonstrated, the incorporation of noble metal centers, the addition of soluble base and use of high temperature regimes are generally required in order to achieve high yields of the target product in a reasonable timescale. Therefore, it is highly demanding as well as challenging for the development of highly efficient noble metal-free heterogeneous catalyst for one-pot cascade reactions without additives (eg. base) under mild conditions.

Polyoxometalates (POMs) are a large class of discrete metal oxide clusters of early transition metals such as V, Mo and W *etc.*, which have been widely applied in catalytic reactions,[16] such as oxidation of alcohols,[17-19] epoxidation of alkenes and alkenols,[20-21] bromination of alkenes[22-23] and water splitting.[24-25] Layered double hydroxides (LDHs)[26] are a series of layered materials with tunable interlayer galleries, with the general formula of $[M^{2+}_{1-x}M^{3+}_{x}(OH)_2](A^{n-})_{x/n}\cdot mH_2O$, where M^{2+} and M^{3+} are di- and tri-valent metal cations, and A^{n-} is a counter anion. It has been demonstrated

that LDHs are effective supports for the immobilization of anionic POM catalysts.[27-30] Indeed, LDHs possess a number of active basic sites that can efficiently catalyze Knoevenagel condensation reactions.[31-33] Hence, it is highly desirable the possibility of designing new bi-functional POM-LDHs catalysts which can promote both oxidation and Knoevenagel condensation reactions in the absence of any other additives under mild conditions.

In this work, we report the preparation of a series of bi-functional catalysts of the general formula, Tris-LDH-$X_4(PW_9)_2$ by intercalating POM anions of $[X_4(H_2O)_2(PW_9O_{34})_2]^{10-}$ (X = Mn, Fe, Co, Ni, Cu and Zn) into a Tris-modified LDH using a facile ion exchange method. Among all the members of this family of catalysts, Tris-LDH-$Zn_4(PW_9)_2$ exhibits the highest activity and selectivity in the cascade reaction of oxidation-Knoevenagel condensation between benzyl alcohol and ethyl cyanoacetate to produce benzylidene ethyl cyanoacetate under mild and soluble-base-free conditions. Finally, the heterogeneous catalysts can be easily recovered and reused for at least ten times without obvious deterioration of their structural integrity and activity due to strong host-guest interaction between the LDHs and POM anions.

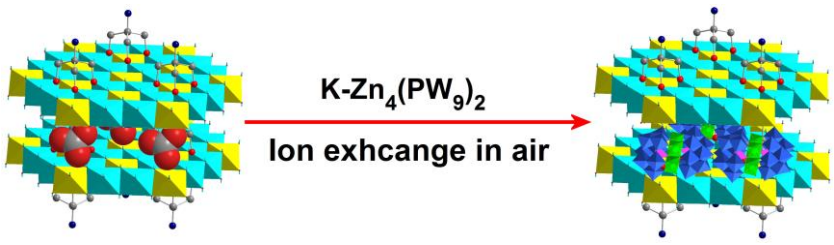

Scheme 1. Schematic representation of the synthetic process for the intercalation of $[Zn_4(H_2O)_2(PW_9O_{34})_2]^{10-}$ into Tris-stabilized LDHs.

Results and discussion

Synthesis and Characterization. Ion exchange of K-$X_4(H_2O)_2(PW_9O_{34})_2$ with Tris-LDH-CO_3 under ambient conditions without the necessity of degassing CO_2 led to the formation of a new intercalated assembly of Tris-LDH-$X_4(PW_9)_2$ (Scheme 1). As shown in Figure 1A, the XRD patterns of Tris-LDH-CO_3 show the characteristic (003), (006), (012), (110) and (113) at 2θ = 11.5°, 23.5°, 34.8°, 61.1°, and 62.4°, respectively. After ion exchange, the characteristic (003), (006) of Tris-LDH-$X_4(PW_9)_2$ shift to 8.5°, 18.3°, indicating that the $[X_4(H_2O)_2(PW_9O_{34})_2]^{10-}$ ions have been successfully intercalated into the interlayer of Tris-modified LDH.

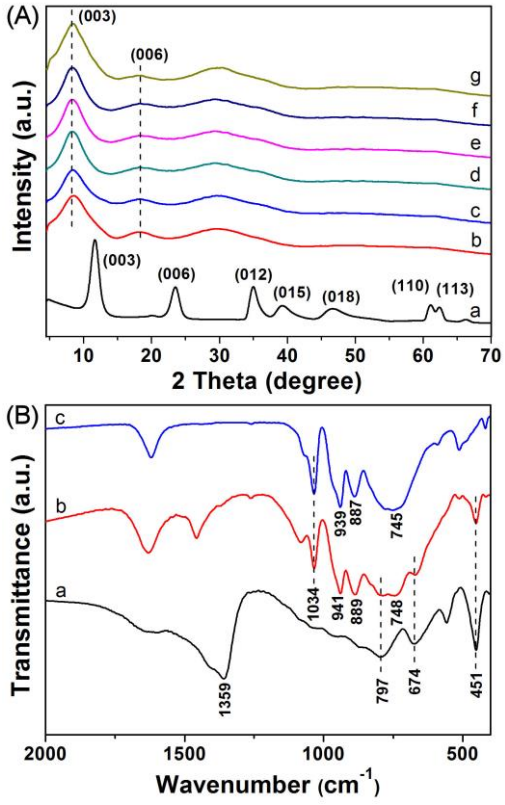

Figure 1. (A) XRD patterns of (a) Tris-LDH-CO_3 and (b-g) Tris-LDH-$X_4(PW_9)_2$ (X = Mn, Fe, Co, Ni, Cu and Zn, respectively), (B) FT-IR spectra of (a) Tris-LDH-CO_3, (b) Tris-LDH-$Zn_4(PW_9)_2$ and (c) K- $[Zn_4(H_2O)_2(PW_9O_{34})_2]^{10-}$.

FT-IR spectrum of $K_{10}[Zn_4(H_2O)_2(PW_9O_{34})_2]$ (denoted as K-$Zn_4(PW_9)_2$) in Figure 2B exhibits peaks at 939, 887 and 745 cm^{-1}, which are attributed to the vibrations of

W–O_t, W–O_c–W and W–O_e–W (t, terminal; c, corner sharing; e, edge sharing),[34] respectively. These W–O stretching bands can be clearly observed in the FT-IR spectrum of Tris-LDH-$Zn_4(PW_9)_2$ slightly shifted to 941, 891 and 748 cm^{-1}, respectively. The observed shift is due to the presence of strong electrostatic interactions and hydrogen bonds formed between the layers of LDHs and the POM anions.[38] The peak at 1034 cm^{-1} in both spectra of K-$Zn_4(PW_9)_2$ and Tris-LDH-$Zn_4(PW_9)_2$ can be assigned to the P-O vibration of the heteroatom within the POM clusters. Additionally, the absorption bands at the range of 400-800 cm^{-1} in both spectra of Tris-LDH-CO_3 and Tris-LDH-$Zn_4(PW_9)_2$ are attributed to O-M-O vibration in the brucite-like layers of LDHs.[35] Meanwhile, the peak at 1359 cm^{-1} of Tris-LDH-CO_3, due to the vibration of CO_3^{2-} anions, disappears in FT-IR spectrum of the composite Tris-LDH-$Zn_4(PW_9)_2$, suggesting the successful ion exchange of CO_3^{2-} anions by POM clusters. The FT-IR spectra of Tris-LDH-$X_4(PW_9)_2$ (X = Mn, Fe, Co, Ni and Cu) are shown in Figure S1.

Additional evidence of the complete exchange of the CO_3^{2-} anions can be seen from the ^{13}C CP/MAS NMR study of Tris and Tris-LDH-CO_3 (Figure 2A). The spectrum exhibits a strong signal at 171.1 ppm, which can be ascribed to the interlayer CO_3^{2-} anions.[35] It is noted that this signal is absent in the ^{13}C CP/MAS NMR spectrum of Tris-LDH-$Zn_4(PW_9)_2$ composite material indicative of the complete ion exchange of the CO_3^{2-} anions by the $[Zn_4(H_2O)_2(PW_9O_{34})_2]^{10-}$ anions during the intercalation process. Furthermore, one set of signals centered at δ = -4.6 ppm can be observed in the ^{31}P NMR spectrum of Tris-LDH-$Zn_4(PW_9)_2$ and K-$Zn_4(PW_9)_2$, indicating that the POM anions have been successfully incorporated into the Tris-modified LDHs (Figure 2B).

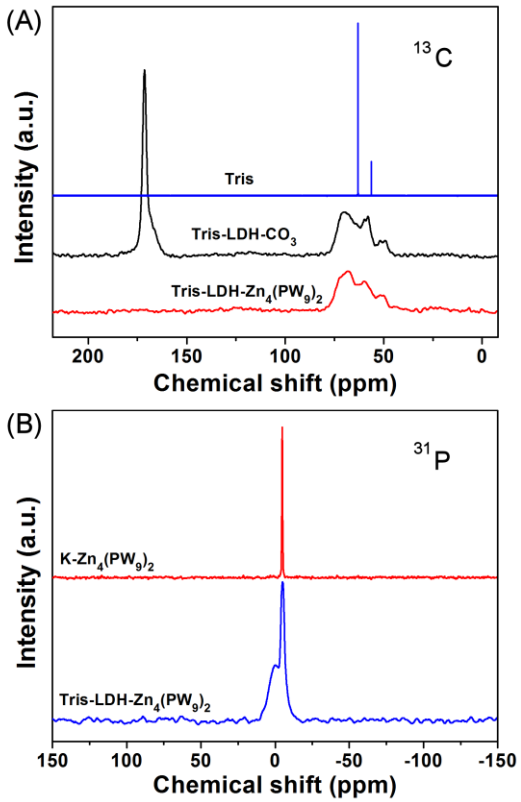

Figure 2. (A) The ^{13}C CP/MAS NMR spectra of Tris, Tris-LDH-CO_3 and Tris-LDH-$Zn_4(PW_9)_2$ and (B) the ^{31}P CP/MAS NMR spectra of K- $Zn_4(PW_9)_2$ and Tris-LDH-$Zn_4(PW_9)_2$.

XPS analysis of the composite Tris-LDH-$Zn_4(PW_9)_2$ is shown in Figure 3. Initial survey of the XPS spectrum showed that the Tris-LDH-$Zn_4(PW_9)_2$ sample is composed of the elements of Mg, Al, Zn, P, and W (Figure 3A). Figures 3B-C present the relevant binding energies of Mg 1s (1303.5 eV) and Al 2p (74.4 eV) due to the presence of the Tris-modified LDH whilst figures 3D-F present the relevant binding energies of Zn 2p, P 2p and W 4f due to the intercalation of the $[Zn_4(H_2O)_2(PW_9O_{34})_2]^{10-}$ clusters in the Tris-LDH-$Zn_4(PW_9)_2$ composite material. Furthermore, the W 4f spectrum (Figure 3F) can be de-convoluted into a doublet consisting of W $4f_{7/2}$ at 35.7 eV and W $4f_{5/2}$ at 37.8 eV, respectively. The doublet is ascribed to the W in the W-O bond configuration and typically can be assigned to the existence W^{6+} centers.[39] This result is in agreement with the oxidation state of the W centers originating from the starting material, K-$Zn_4(PW_9)_2$.

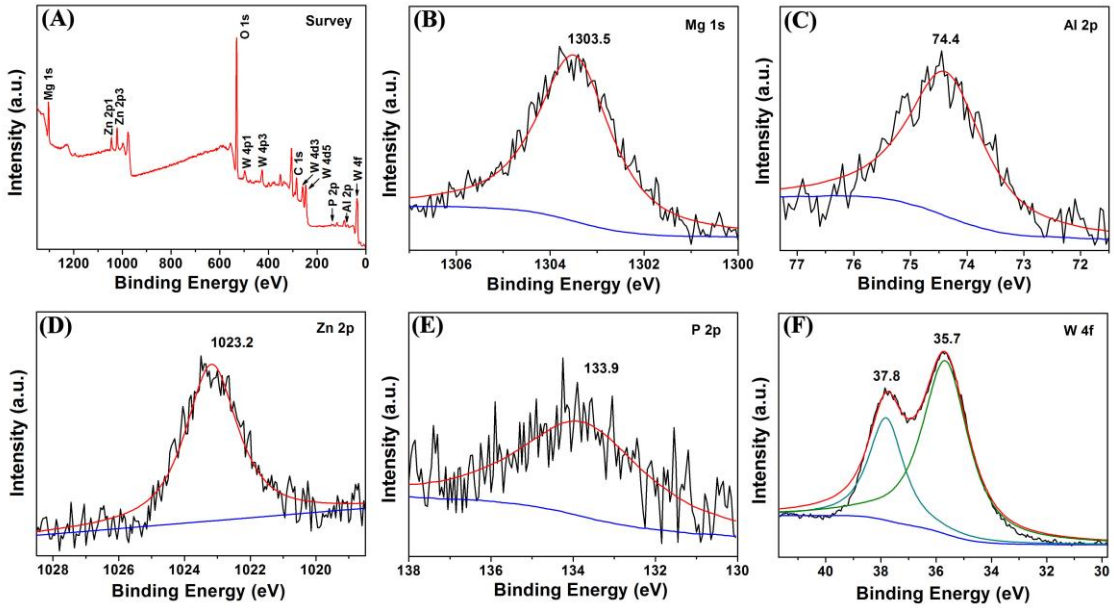

Figure 3. (A) XPS spectra of the Tris-LDH-$Zn_4(PW_9)_2$ sample, (B) Mg 1s, (C) Al 2p, (D) Zn 2p, (E) P 2p, (F) W 4f.

The TG-DTA analysis has been performed for the Tris-LDH-$Zn_4(PW_9)_2$ where two weight-loss stages can be observed as the temperature increases from 32 to 800 °C (Figure 4A). The first weight loss of 7.23% occurs between 40 and 244 °C, which can be attributed to the removal of water molecules absorbed in the surface and the interlayer space of the Tris-LDH-$Zn_4(PW_9)_2$ composite. The second weight loss step of 8.74% at 244-800 °C corresponds to the decomposition of Tris molecules and subsequent disintegration of the layered structure. Based on the TG-DTA and elemental analysis considerations (Mg = 8.071%, Al = 4.483%, W = 54.692% and N = 0.644%), the elemental composition of the composite material can be identified as: $Mg_{0.66}Al_{0.33}(C_4H_8NO_3)_{0.092}(OH)_{1.71}Zn_{0.132}(PW_9O_{34})_{0.066}\cdot 0.87H_2O$ (Table S1). The TG analysis plots of K-$Zn_4(PW_9)_2$ and Tris-LDH-CO_3 are shown in Figure S2 for comparison.

BET measurement has been carried out on the Tris-LDH-CO_3 and Tris-LDH-$Zn_4(PW_9)_2$, in order to obtain more detailed information on the structural features of

the as-prepared material. The specific surface area, pore volume, and average pore diameter (estimated from N_2 adsorption–desorption isotherms) are reported in Table S2. Tris-LDH-CO_3 and Tris-LDH-$Zn_4(PW_9)_2$ display H4 type hysteresis loops (Figure 4B), indicating that the pores are produced by the aggregation of slit-shaped microsized pores.[40]

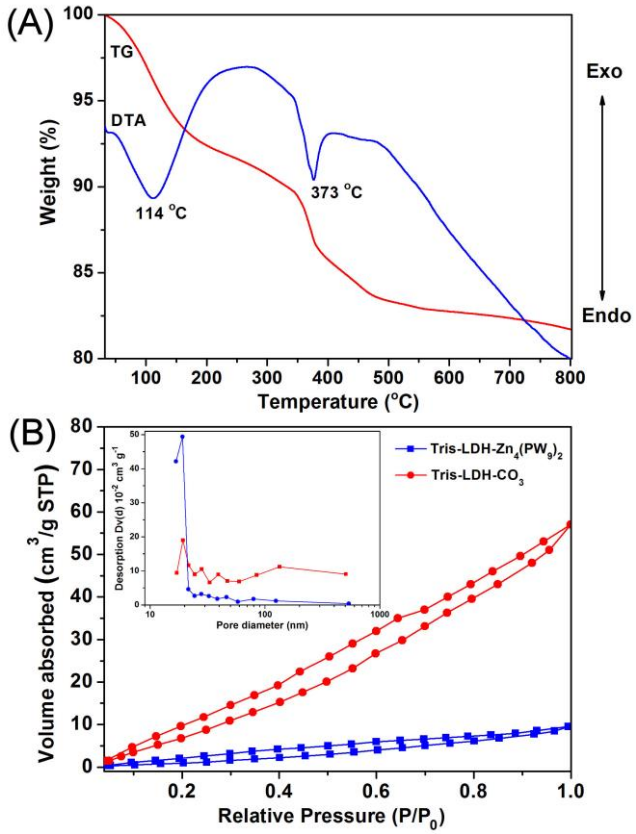

Figure 4. (A) TG-DTA of Tris-LDH-$Zn_4(PW_9)_2$ and (B) Adsorption–desorption isotherms of Tris-LDH-CO_3, Tris-LDH-$Zn_4(PW_9)_2$.

SEM analysis (Figure S2) shows that the plate sizes of Tris-LDH-$Zn_4(PW_9)_2$ are in the range of 20~30 nm. HRTEM images of the Tris-LDH-$Zn_4(PW_9)_2$ are shown in Figure 5. The observed homogeneously distributed dark dots of ~1 nm diameter size in the samples of Tris-LDH-$Zn_4(PW_9)_2$ can be ascribed to the intercalated POM species. EDX studies (Figure 5D) conducted on the dark areas identified from the HRTEM images revealed the presence of Mg, Al, Zn, P, W, C and N, which provides further support for the composition of the Tris-LDH-$Zn_4(PW_9)_2$.

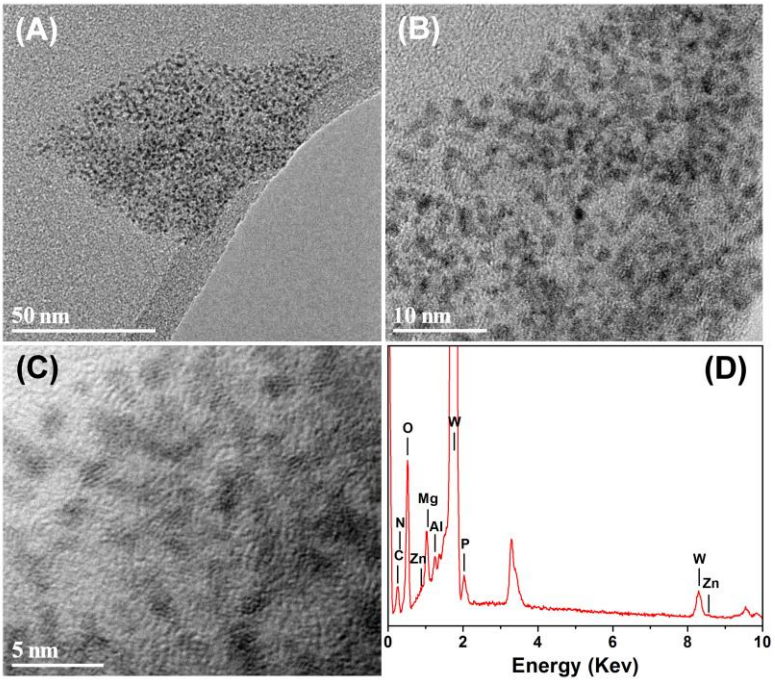

Figure 5. (A), (B) and (C) HRTEM images of Tris-LDH-$Zn_4(PW_9)_2$; (D) EDX of Tris-LDH-$Zn_4(PW_9)_2$.

The CO_2-TPD measurement of Tris-LDH-$Zn_4(PW_9)_2$, Mg_2Al-$Zn_4(PW_9)_2$ and Zn_2Al-$Zn_4(PW_9)_2$ are outlined in Figure 6. It is demonstrated that all these samples display three kinds of CO_2 desorption peaks, which can be ascribe to weak basic sites centered at 90-153 ^oC, moderate basic sites centered at 164-227 ^oC and strong basic sites ranging from 252-373 ^oC. In comparison with Mg_2Al-$Zn_4(PW_9)_2$ and Zn_2Al-$Zn_4(PW_9)_2$, Tris-LDH-$Zn_4(PW_9)_2$ contains larger amount of basic sites, particularly of the stronger ones. It is worth noting that Tris-LDH-$Zn_4(PW_9)_2$ has a much higher basic site density than that of Mg_2Al-$Zn_4(PW_9)_2$ and Zn_2Al-$Zn_4(PW_9)_2$ based on the data summarized in (Table 1). In addition, Zn_2Al-$Zn_4(PW_9)_2$ possess the lowest basic site density among the three samples.

Table 1. Results of temperature-programmed desorption of CO_2 for the studied samples

sample	specific basicity (CO_2 μmol·g^{-1})[a]			
	total	W.	M.	S.
Zn_2Al-$Zn_4(PW_9)_2$	248	146.5(59.1)[b]	54.7(23.0)	46.8(18.9)
Mg_2Al-$Zn_4(PW_9)_2$	305	158.3(51.9)	13.6(4.5)	133.1(43.6)
Tris-LDH-$Zn_4(PW_9)_2$	614	134.1(21.8)	12.3(2.0)	467.6(76.2)

[a]W.: weak basic sites; M.: moderate basic sites; S.: strong basic sites. [b]Relative amounts of the basic sites (%).

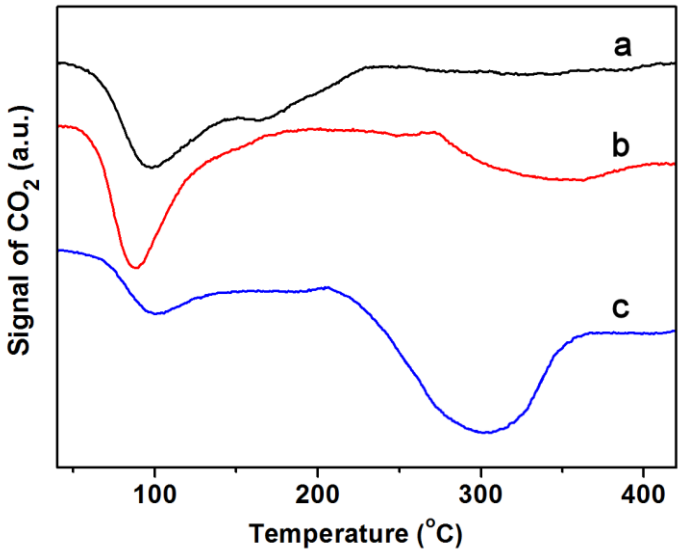

Figure 6. CO_2-TPD curves of (a) Zn_2Al-$Zn_4(PW_9)_2$, (b) Mg_2Al-$Zn_4(PW_9)_2$ and (c) Tris-LDH-$Zn_4(PW_9)_2$

Cascade catalytic reaction. The performance and efficacy of the Tris-LDH-$Zn_4(PW_9)_2$ composite as bi-functional heterogeneous catalyst was tested in the conversion of benzyl alcohol (**A1**) to benzylidene ethyl cyanoacetate (**C1**) in an one-pot cascade reaction. The cascade reaction involves two separate steps: 1) oxidation of benzyl alcohol to benzaldehyde (**B1**) by POM anions in the presence of H_2O_2 and 2) Knoevenagel condensation between benzaldehyde and ethyl cyanoacetate promoted by the basic sites of the LDHs. The catalytic performance of a series of control experiments has been also investigated for comparison and the results are summarized in Table 2.

The cascade reaction proceeds smoothly with 99% conversion and ≥99% selectivity using the Tris-LDH-$Zn_4(PW_9)_2$ catalyst (Table 2, entry 6). The control samples of Tris-LDH-$X_4(PW_9)_2$ (X = Mn, Fe, Co, Ni and Cu) show quite lower conversion of **A1** (Table 1, entries 1-5), indicating that the POM anions hosted in the Tris-modified LDH play an important role for the efficient oxidation of **A1** during the first step of the reaction. When Mg_2Al-$Zn_4(PW_9)_2$ and Zn_2Al-$Zn_4(PW_9)_2$ are used instead, the relevant conversion values for **A1** found to be nearly the same; however, the relevant yields regarding the condensation step towards the formation of **C1** found to be significantly lower (Table 2, entries 7-8) due to the lower basicity of the conventional LDH support compared to the one observed in Tris-modified LDH. It is worth noting that Zn_2Al-$Zn_4(PW_9)_2$ exhibits a much lower yield for **C1** than that of Mg_2Al-$Zn_4(PW_9)_2$ due to the lower basicity of the former composite. Investigation of the catalytic efficacy of the mono-functional catalysts, shows that neither K-$Zn_4(PW_9)_2$ nor Tris-LDH-CO_3 can convert **A1** into the target product **C1** (Table 2, entries 9-10). Finally, the physical mixture of Tris-LDH-CO_3 and K-$Zn_4(PW_9)_2$ with comparable active site concentrations shows inferior efficacy (Table 2, entry 11), as both the activity and selectivity are considerably lower than those observed in the case of the bi-functional catalyst Tris-LDH-$Zn_4(PW_9)_2$, demonstrating the advantages of the proposed POM-intercalated catalyst design. In comparison with Tris-LDH-$Zn_4(PW_9)_2$, the reported Pd/zeolites[41] based catalyst exhibits a much lower conversion and lower selectivity for the same cascade reaction. Moreover, the performance of the Zr-MOF-NH_2 catalyst[42], for the same cascade reaction found to be quite sluggish.

Table 2. Performance of different catalysts in the oxidation of benzyl alcohol and the subsequent Knoevenagel condensation with ethyl cyanoacetate[a]

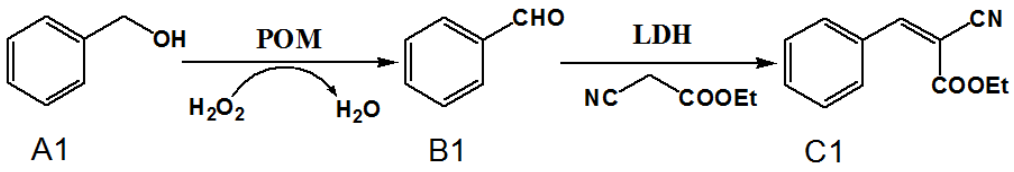

Entry	Catalyst	Conversion A1 (%)	Yield B1 (%)	Yield C1 (%)	TON[b]
1	Tris-LDH-$Mn_4(PW_9)_2$	12	0	12	12
2	Tris-LDH-$Fe_4(PW_9)_2$	20	0	20	20
3	Tris-LDH-$Co_4(PW_9)_2$	29	0	29	29
4	Tris-LDH-$Ni_4(PW_9)_2$	25	0	25	25
5	Tris-LDH-$Cu_4(PW_9)_2$	47	0	47	47
6	Tris-LDH-$Zn_4(PW_9)_2$	99	0	99	99
7	Mg_2Al-$Zn_4(PW_9)_2$	95	13	82	82
8	Zn_2Al-$Zn_4(PW_9)_2$	94	33	61	61
9	K-$Zn_4(PW_9)_2$	100	92	8	8
10	Tirs-LDH-CO_3	Trace	Trace	Trace	Trace
11	K-$Zn_4(PW_9)_2$ + Tirs-LDH-CO_3	83	31	52	52
12[c]	Pd/Zeolites	87	48	39	—
13[d]	Zr-MOF-NH_2	100	2	98	—
14	none	0	0	0	—

[a]Reaction conditions: catalyst (0.01 mmol), **A1** (1 mmol), ethyl cyanoacetate (3 mmol), H_2O_2 (1 mL), CH_3CN (3 mL), T = 353 K, 6h. [b]TON = moles of product **C1**/moles of catalyst used. [c]Ref. 41: T = 358 K, 15h. [d]Ref. 42: T = 363 K, 48h.

In order to identify the best solvent medium for the cascade reaction, we investigate the effect of a series of solvents on the catalytic efficacy; the results are summarized in Table 3. The cascade reaction proceeds efficiently when CH_3OH and C_2H_5OH are used as solvents where the conversion of **A1** reaches 93 % and 92 %, respectively (Table 3, entries 1 and 2). When CH_3CN is used instead, we observe almost complete conversion of **A1** (99 %) and selectivity for the final product, **C1** (100 %). In contrast, the catalytic activity and selectivity decrease dramatically when THF, toluene, DMF, DMSO and H_2O are used as solvents in the cascade reaction (Table 3, entries 4-8).

Based on the above screening, we selected CH_3CN as the most appropriate solvent medium.

Table 3. Effect of different solvents on the oxidation of benzyl alcohol and the subsequent Knoevenagel condensation with ethyl cyanoacetate[a]

Entry	Catalyst	Conversion A1 (%)	Yield B1 (%)	Yield C1 (%)	TON[b]
1	CH_3OH	93	0	93	93
2	C_2H_5OH	92	0	92	92
3	CH_3CN	99	0	99	99
4	THF	78	16	62	62
5	Toluene	84	9	75	75
6	DMF	89	4	85	85
7	DMSO	66	12	44	44
8	H_2O	47	8	39	39

[a]Reaction conditions: Tris-LDH-$Zn_4(PW_9)_2$ (0.01 mmol), **A1** (1 mmol), ethyl cyanoacetate (3 mmol), H_2O_2 (1 mL), solvent (3 mL), T = 353 K, 6h. [b]TON = moles of product **C1**/moles of catalyst used.

The catalytic reaction pathway has been explored by tracing the product distribution change as a function of the reaction time using Tris-LDH-$Zn_4(PW_9)_2$ as catalyst. Figure 7A shows the evolution with time of the different products obtained when benzyl alcohol and ethyl cyanoacetate were reacted in the presence of the bi-functional catalyst. Initially, the benzaldehyde can be obtained via oxidation of benzyl alcohol by the POM clusters in the presence of H_2O_2. Simultaneously, in the presence of the basic sites of Tris-modified LDH, ethyl cyanoacetate is activated to give a nucleophile which rapidly condenses with benzaldehyde leading to the formation of the condensation product, benzylidene ethyl cyanoacetate. It should be noted that the yield of benzaldehyde increases initially as a function of the reaction time and then decreases slowly after 1 h due to subsequent conversion to the condensation product (**C1**), which

is a typical behaviour for a tandem reaction. The schematic reaction profile is illustrated in Scheme 2.

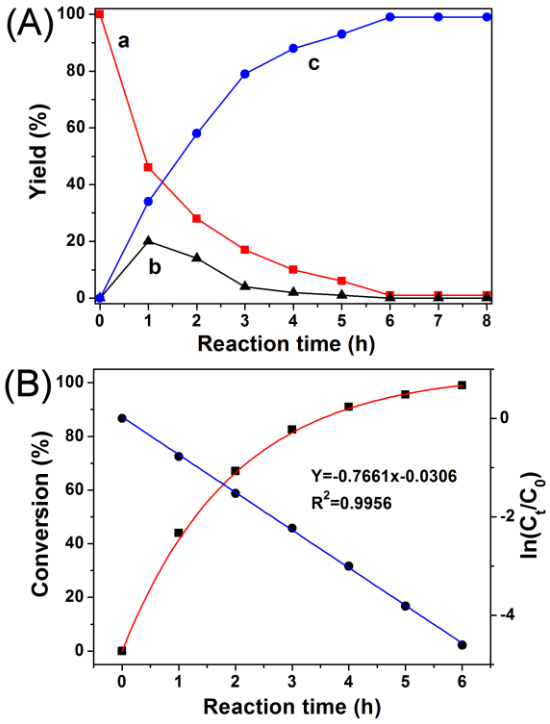

Figure 7. (A) Reaction profile of oxidation-Knoevenagel condensation of benzyl alcohol and ethyl cyanoacetate. (a) **A1** (black), (b) **B1** (red) and (c) **C1** (blue). (B) Kinetic study for conversion of **A1** by Tris-LDH-$Zn_4(PW_9)_2$. Reaction conditions: Tris-LDH-$Zn_4(PW_9)_2$ (0.01 mmol), **A1**(1 mmol), ethyl cyanoacetate (3 mmol), H_2O_2 (1 mL), solvent (3 mL), T = 353 K, 6 h.

The kinetic study for conversion of **A1** by Tris-LDH-$Zn_4(PW_9)_2$ has been illustrated in Figure 7B. Percentage of conversion and $\ln(C_t/C_0)$ are plotted against reaction time, in which C_0 and C_t are initial **A1** concentration and the concentration at time t, respectively. The linear fit of the data demonstrates that the catalytic reaction exhibits pseudo-first-order kinetics for the conversion of **A1** (R^2=0.9956). The rate constant k of the conversion of **A1** can be determined to be 0.7661 h^{-1}.

$$-\frac{dC_t}{dt} = k \qquad (1)$$

$$\ln(\frac{C_0}{C_t}) = kt \qquad (2)$$

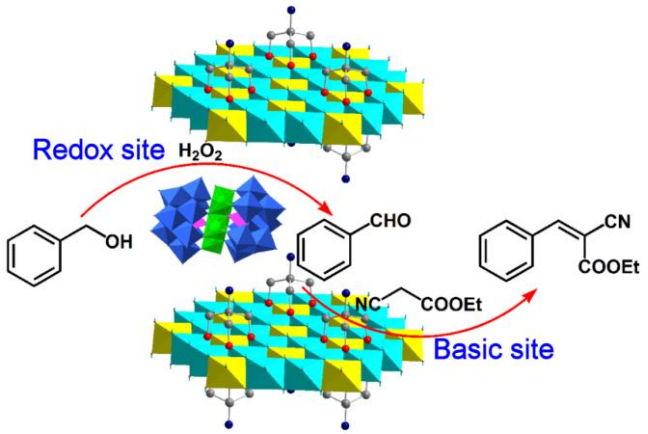

Scheme 2. Reaction pathway of the oxidation-Knoevenagel condensation reaction by Tris-LDH-$Zn_4(PW_9)_2$.

In an effort to test the general applicability and efficacy of the Tris-LDH-$Zn_4(PW_9)_2$ heterogeneous catalyst in cascade reactions involving different substrates, we have studied the conversion of a series of substituted benzyl alcohols (**A**) and active methylene compounds (**B**); the obtained results are summarized in Table 3. The data demonstrates that the introduction of electron donor groups at the *para* position of the benzyl alcohol lead to high yields of the target product (**C**) (Table 4, entries 2-4) after prolonged reaction time; on the other hand, electron withdrawing groups at the *para* position, exhibit decreased yields for the final condensation product (**C**) (Table 4, entries 5-8). Specifically in the case of 2,6-difluorobenzyl alcohol, a much lower conversion of **A** and selectivity for **C** is observed (Table 4, entry 9), which can be attributed to the net electron withdrawing effect and the increased steric hindrance of the bulky groups in **A**. When malononitrile is used as the condensation reactant, the whole cascade reaction proceeds fast to completion within 4 hours (Table 4, entry 10). On the contrary, the yields for the final product (**C**) are moderately to significantly lower in the cases of diethyl malonate and phenylacetonitrile, respectively (Table 4, entries 11-12). Malononitrile is the most active methylene compound among the substrates used in this work which is reflected to the observed differences in the yields for **C** in the cascade reaction.

Table 4. One-pot oxidation-Knoevenagel cascade reactions towards different substrates using Tris-LDH-$Zn_4(PW_9)_2$ as the catalyst[a]

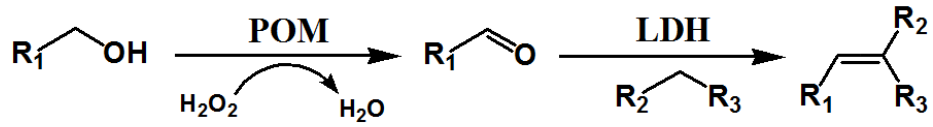

A B C

Entry	R_1	R_2	R_3	Time (h)	Conversion A (%)	Yield B (%)	Yield C (%)	TON[b]
1	C_6H_5	CN	COOEt	6	99	0	99	99
2	4-CH_3-C_6H_5	CN	COOEt	16	92	0	92	92
3	4-CH_3O-C_6H_5	CN	COOEt	24	93	0	93	93
4	4-NH_2-C_6H_5	CN	COOEt	24	90	0	90	90
5	4-F-C_6H_5	CN	COOEt	24	86	0	86	86
6	4-Cl-C_6H_5	CN	COOEt	24	83	0	83	83
7	4-Br-C_6H_5	CN	COOEt	24	79	0	79	79
8	4-NO_2-C_6H_5	CN	COOEt	24	60	0	60	60
9	2,6-2F-C_6H_5	CN	COOEt	24	48	16	32	32
10	C_6H_5	CN	CN	4	99	0	99	99
11	C_6H_5	COOEt	COOEt	16	99	7	92	92
12	C_6H_5	C_6H_5	CN	24	99	25	64	64

[a]Reaction conditions: Tris-LDH-$Zn_4(PW_9)_2$ (0.01 mmol), alcohol (1 mmol), active methylene compounds (3 mmol), H_2O_2 (1 mL), $CNCH_3$ (3 mL), T = 353 K. [b]TON = moles of product **C**/moles of catalyst used.

In order to evaluate the stability of the composite material, identify potential leaching issues and demonstrate the heterogeneous nature of the Tris-LDH-$Zn_4(PW_9)_2$ composite material, we have designed the following experimental procedure. After allowing the benzyl alcohol and ethyl cyanoacetate to react for 2 h, we removed the catalyst from the reaction vessel by filtration whilst the conversion of benzyl alcohol and the yield of the condensation product at this point reached the values of 72% and 58 %, respectively (Figure 8A). The reaction mixture was kept under stirring for another 4 h under the same experimental conditions while we kept monitoring any concentration changes of the species. The obtained data (Figure 8A) demonstrate that the removal of the solid catalyst, Tris-LDH-$Zn_4(PW_9)_2$ from the reaction mixture, brings the cascade reaction, and as a consequence the conversion of benzyl alcohol and

the yield of the target product, to a halt. In addition, ICP measurements of the filtrate after removing the catalyst indicate that there is no evidence of W content in the filtrate. These two experimental results provide unambiguous proof that there is no leaching of POM clusters from the Tris-LDH-$Zn_4(PW_9)_2$ composite into the solution during the course of the cascade reaction. This can be attributed to the multiple electrostatic and H-bonding interactions between Tris-modified LDH and POM anions in the two-dimensional restricted region.

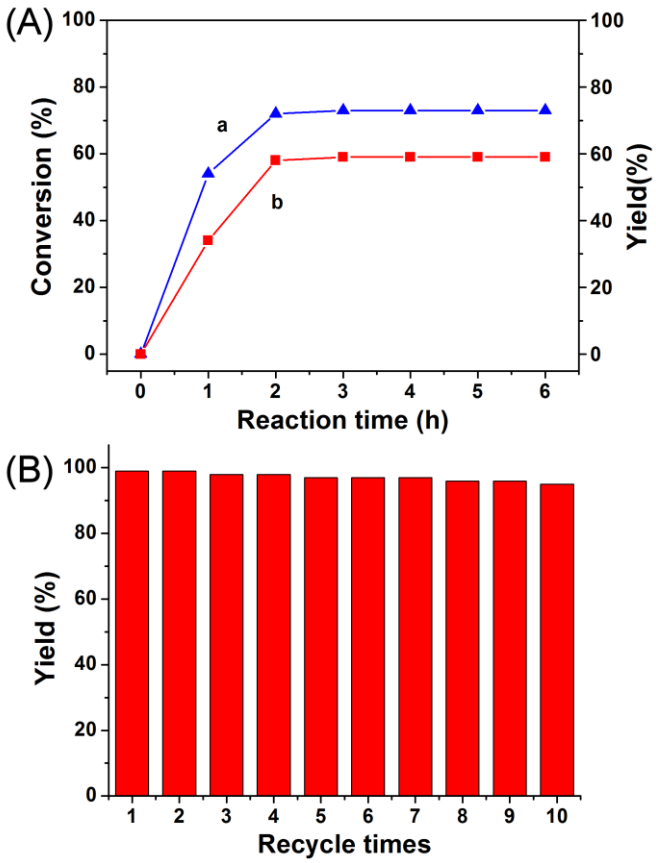

Figure 8. (A) Leaching test for the cascade reaction of benzyl alcohol with ethyl cyanoacetate over Tris-LDH-$Zn_4(PW_9)_2$. (a) conversion of benzyl alcohol and (b) yield of benzylidene ethyl cyanoacetate. Reaction conditions: benzyl alcohol (1 mmol), ethyl cyanoacetate (1.5 mmol), H_2O_2 (1 mL), solvent (3 mL), catalyst (0.01 mmol), T = 353 K. (B) Recycling test of the Tris-LDH-$Zn_4(PW_9)_2$ catalyst for 10 times.

Most importantly, the heterogeneous catalyst can be successfully recovered upon completion of the cascade reaction by filtration. As shown in Figure 8B, the Tris-LDH-

$Zn_4(PW_9)_2$ composite used for the promotion of the cascade reaction can be easily recovered by filtration and recycled for at least 10 times without obvious deterioration of its catalytic activity. In addition, the characterization of the recycled catalyst using XRD, FT-IR, ^{31}P NMR and XPS demonstrated the retention of its structural integrity (Figure S4).

Conclusions

In conclusion, a series of bi-functional catalysts of the general formula Tris-LDH-$X_4(PW_9)_2$ (X = Mn, Fe, Co, Ni, Cu and Zn) have been fabricated by intercalating the POM anions into Tris-modified LDH following a facile ion exchange method. The experimental results show for the first time the efficient utilization of POM-LDH composite materials as bi-functional heterogeneous catalysts for the promotion of cascade reactions. The combinatorial effect of this family of composite materials was demonstrated by the fine tuning of the oxidation catalyst (POM) and the basicity of the LDH layers (Knoevenagel condensation). More specifically, the Tris-LDH-$Zn_4(PW_9)_2$ composite exhibited excellent activity and selectivity under mild and soluble-base-free conditions in the cascade oxidation-Knoevenagel condensation reaction of various substituted benzyl alcohol and active methylene substrates. This work renders the POM-intercalated LDHs as very attractive low cost, energy efficient and noble metal-free alternative catalysts. Moreover, the reported heterogeneous catalysts can be easily recovered upon completion of the cascade reaction and recycled for at least ten times without measurable deterioration of their catalytic activity or structural integrity. This new approach opens up endless possibilities for the engineering of low cost, environmentally friendly and modular multi-functional POM-LDH catalysts, tailored for the promotion of specific cascade reactions. Our current research effort is focused

on exploring the potential of the family of POM-LDHs based multi-functional catalysts.

Experimental section

Chemicals. $MgCl_2·6H_2O$, $AlCl_3·6H_2O$, $Zn(NO_3)_2·6H_2O$, $MnCl_2·2H_2O$, $FeCl_3·6H_2O$, $Co(NO_3)_2·6H_2O$, $Ni(NO_3)_3·6H_2O$, $CuCl_2·2H_2O$, $Al(NO_3)_3·9H_2O$, Na_2CO_3, $NaWO_4·2H_2O$, H_3PO_4, CH_3COOH, KCl, tris(hydroxymethyl)aminomethane (tris), benzyl alcohol, 4-methylbenzyl alcohol, 4-methoxybenzyl alcohol, 4-fluorobenzyl alcohol, 4-chlorobenzyl alcohol, 4-bromobenzylalcohol, 4-aminobenzyl alcohol, 4-nitrobenzyl alcohol, 2,6-difluorobenzyl alcohol, ethyl cyanoacetate, malononitrile, diethyl malonate and phenylacetonitrile were purchased from *Sigma-Aldrich* and used without any further purification. All solvents were of analytical grade, purchased from Alfa Aesar and used without further purification.

Preparation of Tris-LDH-$Zn_4(PW_9)_2$. $K_{10}[Zn_4(H_2O)_2(PW_9O_{34})_2]·20H_2O$[34] (K-$Zn_4(PW_9)_2$) and the tripodal ligand-stabilized layered double hydroxide (Tris-LDH-CO_3)[35] were synthesized according to previously reported methodologies. The POMs were intercalated into Tris-LDH-CO_3 using an anion-exchange method[36] under CO_2-existing conditions. Tris-LDH-CO_3 (2 mg/mL) was then re-dispersed in a solution of $K_{10}[Zn_4(H_2O)_2(PW_9O_{34})_2]$ (0.1 M) and stirred for 2 h at room temperature. The precipitate was then filtered, washed with water and acetone and dried in an oven to obtain the Tris-LDH-$Zn_4(PW_9)_2$ composite.

Preparation of Tris-LDH-$X_4(PW_9)_2$ (X = Mn, Fe, Co, Ni, Cu), Mg_2Al-$Zn_4(PW_9)_2$, and Zn_2Al-$Zn_4(PW_9)_2$. Tris-LDH-$X_4(PW_9)_2$ (X = Mn, Fe, Co, Ni, Cu) were fabricated following the same synthetic procedure according to the literature.[34-36] Mg_2Al-CO_3 and

$Mg_2Al\text{-}NO_3$,[37] $Mg_2Al\text{-}Zn_4(PW_9)_2$,[30] and $Zn_2Al\text{-}CO_3$, and $Zn_2Al\text{-}NO_3$[29] were synthesized according to previously reported literature method.

One-pot oxidation–Knoevenagel condensation reaction. 0.01 mmol solid catalyst, 1 mmol benzyl alcohol, 1.5 mmol ethyl cyanoacetate, 1 mL 30 wt% H_2O_2 aqueous solution and 3 mL acetonitrile were mixed in a 20 mL glass bottle at 80 °C and the reaction mixture was kept under vigorous stirring. The reaction mixtures were effectively quenched after 6 h. The resulting oily products were extracted with diethyl ether and analyzed by gas chromatography equipped with a flame ionization detector (GC-FID). The conditions were as follows: injection port temperature 340 °C; detector temperature 340 °C; oven temperature 70 °C; carrier gas: ultrapure nitrogen; sample injection volume 1 mL.

Characterization. Powder X-ray diffraction (XRD) patterns were recorded on a Rigaku XRD-6000 diffractometer under the following conditions: 40 kV, 30 mA, Cu Kα radiation (λ = 0.154 nm). FT-IR spectra were recorded on a Bruker Vector 22 infrared spectrometer using KBr pellets. The solid state NMR experiments were carried out at 75.6 MHz for ^{13}C and at 121.0 MHz for ^{31}P on a Bruker Avance 300M solid-state spectrometer equipped with a commercial 5 mm MAS NMR probe. The N_2 adsorption-desorption isotherms were measured using a Quantachrome Autosorb-1 system at the liquid nitrogen temperature, and the samples were degassed at 120 °C for 6 hours before the measurements. HRTEM images were conducted on a JEOL JEM-2010 electron microscope operating at 200 kV. Scanning electron microscopy (SEM) images were obtained using a Zeiss Supra 55 SEM. Thermogravimetric and differential thermal analyses (TG-DTA) were performed on a TGA/DSC 1/1100 SF from Mettler Toledo in flowing N_2 with a heating rate of 10 °C min^{-1} from 32 °C to 800 °C. X-ray photoelectron spectroscopy (XPS) measurements were performed on a PHI Quantera

SXM using monochromatized Al K_α exciting X-radiation. The basicity of the composites were probed by the temperature-programmed desorption of carbon dioxide (CO_2-TPD) using a Thermo Electron Corporation TPDRO 1100 analyzer. The samples (100 mg) were degassed by heating at 100^{o}C for 2 h under a He stream (50 mL/min) and then treated with CO_2 stream (40 mL/min) at 50 ^{o}C for 1 h. Physically adsorbed CO_2 was removed by a flushing He stream at the saturation temperature for 2 h. Chemisorbed CO_2 was desorbed by heating from the saturation temperature up to 600 ^{o}C at a rate of 10^{o}C/min. Inductively coupled plasma-atomic emission spectroscopy (ICP-AES, Shimadzu ICPS-7500) was used to measure the concentration of W in the catalysts. GC analyses were performed on an Agilent 7820A GC system using a 30 m 5% phenylmethyl silicone capillary column with an ID of 0.32 mm and 0.25 mm coating (HP-5).

Acknowledgements

This work was supported by National Basic Research Program (2014CB932104), National Science Foundation of China (U1407127), the Fundamental Research Funds for the Central Universities (RC1302, YS1406, XK1530) and Beijing Engineering Centre for Hierarchical Catalysts. H.N.M acknowledges the financial support from University of Glasgow, Royal Society of Edinburgh and Marie Curie actions scheme.

Keywords: Cascade reaction; Polyoxometalate; Layered double hydroxides; Bi-functional catalyst; Heterogeneous catalyst

References

[1] A. Corma, T. Ródenas, M.J. Sabater, *J. Catal.* **2011**, *279*, 319-327.

[2] P. Li, C.Y. Cao, Z. Chen, H. Liu, Y. Yu, W.G. Song, *Chem. Commun.* **2012**, *48*, 10541-10543.

[3] P. Liu, C. Li, E.J. Hensen, *Chem. Eur. J.* **2012**, *18*, 12122-12129.

[4] H. Yang, L. Fu, L. Wei, J. Liang, B.P. Binks, *J. Am. Chem. Soc.* **2015**, *137*, 1362-1371.

[5] D.E. Fogg, E.N. dos Santos, *Coord. Chem. Rev.* **2004**, *248*, 2365-2379.

[6] J.C. Wasilke, S.J. Obrey, R.T. Baker, G.C. Bazan, *Chem. Rev.* **2005**, *105*, 1001-1020.

[7] F.X. Felpin, E. Fouquet, *ChemSusChem* **2008**, *1*, 718-724.

[8] M.J. Climent, A. Corma, S. Iborra, *Chem. Rev.* **2011**, *111*, 1072-1133.

[9] F.X. Zhu, W. Wang, H.X. Li, *J. Am. Chem. Soc.* **2011**, *133*, 11632-11640.

[10] D.B. Ramachary, S. Jain, *Org. Biomol. Chem.* **2011**, *9*, 1277-1300.

[11] Y. Jiang, X.Y. Tang, M. Shi, *Chem. Commun.* **2015**, *51*, 2122-2125.

[12] E. Taarning, A.T. Madsen, J.M. Marchetti, K. Egeblad, C.H. Christensen, *Green Chem.* **2008**, *10*, 408-414.

[13] L. Zhang, W. Wang, A. Wang, Y. Cui, X. Yang, Y. Huang, X. Liu, W. Liu, J.-Y. Son, H. Oji, T. Zhang, *Green Chem.* **2013**, *15*, 2680.

[14] M. Zhao, K. Deng, L. He, Y. Liu, G. Li, H. Zhao, Z. Tang, *J. Am. Chem. Soc.* **2014**, *136*, 1738-1741.

[15] J. Wang, M. Zhu, X. Shen, S. Li, *Chem. Eur. J.* **2015**, *21*, 7532-7539.

[16] H.N. Miras, J. Yan, D.L. Long, L. Cronin, *Chem. Soc. Rev.* **2012**, *41*, 7403-7430.

[17] G. Chen, Y. Zhou, Z. Long, X. Wang, J. Li, J. Wang, *ACS Appl. Mater. Interfaces* **2014**, *6*, 4438-4446.

[18] Y. Chen, R. Tan, W. Zheng, Y. Zhang, G. Zhao, D. Yin, *Catal. Sci. Technol.* **2014**, *4*, 4084-4092.

[19] M.R. Farsani, B. Yadollahi, *J. Mol. Catal. A: Chem.* **2014**, *392*, 8-15.

[20] R. Neumann, M. Dahan, *Nature* **1997**, *388*, 353-355.

[21] Y. Nakagawa, K. Kamata, M. Kotani, K. Yamaguchi, N. Mizuno, *Angew. Chem., Int. Ed.* **2005**, *44*, 5136-5141.

[22] S. Mallik, K.M. Parida, S.S. Dash, *J. Mol. Catal. A: Chem.* **2007**, *261*, 172-179.

[23] K. Yonehara, K. Kamata, K. Yamaguchi, N. Mizuno, *Chem. Commun.* **2011**, *47*, 1692-1694.

[24] Q. Yin, J.M. Tan, C. Besson, Y.V. Geletii, D.G. Musaev, A.E. Kuznetsov, Z. Luo, K.I. Hardcastle, C.L. Hill, *Science* **2010**, *328*, 342-345.

[25] F.M. Toma, A. Sartorel, M. Iurlo, M. Carraro, P. Parisse, C. Maccato, S. Rapino, B.R. Gonzalez, H. Amenitsch, T. Da Ros, L. Casalis, A. Goldoni, M. Marcaccio, G. Scorrano, G. Scoles, F. Paolucci, M. Prato, M. Bonchio, *Nat. Chem.* **2010**, *2*, 826-831.

[26] J. Han, Y. Dou, M. Wei, D.G. Evans, X. Duan, *Angew. Chem., Int. Ed.* **2010**, *49*, 2171-2174.

[27] P. Liu, H. Wang, Z. Feng, P. Ying, C. Li, *J. Catal.* **2008**, *256*, 345-348.

[28] P. Liu, C. Wang, C. Li, *J. Catal.* **2009**, *262*, 159-168.

[29] S. Zhao, J. Xu, M. Wei, Y.-F. Song, *Green Chem.* **2011**, *13*, 384-389.

[30] S. Zhao, L. Liu, Y.F. Song, *Dalton Trans.* **2012**, *41*, 9855-9858.

[31] E. Angelescu, O.D. Pavel, R. Bîrjega, R. Zăvoianu, G. Costentin, M. Che, *Appl. Catal., A* **2006**, *308*, 13-18.

[32] M. Yang, J. Liu, Z. Chang, G.R. Williams, D. O'Hare, X. Zheng, X. Sun, X. Duan, *J. Mater. Chem.* **2011**, *21*, 14741.

[33] Y. Kuwahara, K. Tsuji, T. Ohmichi, T. Kamegawa, K. Mori, H. Yamashita, Waste-slag hydrocalumite and derivatives as heterogeneous base catalysts, *ChemSusChem* **2012**, *5*, 1523-1532.

[34] R.G. Finke, M.W. Droege, P.J. Domaille, *Inorg. Chem.* **1987**, *26* 3886-3896.

[35] Y. Kuroda, Y. Miyamoto, M. Hibino, K. Yamaguchi, N. Mizuno, *Chem. Mater.* **2013**, *25*, 2291-2296.

[36] Y. Chen, D. Yan, Y.F. Song, *Dalton Trans.* **2014**, *43*, 14570-14576.

[37] N. Iyi, Y. Ebina, T. Sasaki, *J. Mater. Chem.* **2011**, *21*, 8085-8095.

[38] Y. Dou, J. Han, T. Wang, M. Wei, D.G. Evans, X. Duan, *Langmuir* **2012**, *28*, 9535-9542.

[39] L. Salvati, L.E. Makovsky, J.M. Stencel, F.R. Brown, D.M. Hercules, *J. Phys. Chem.* **1981**, *85*, 3700-3707.

[40] B.J. Aronson, C.F. Blanford, A. Stein, *Chem. Mater.* **1997**, *9*, 2842-2851.

[41] L. Xu, C.-g. Li, K. Zhang, P. Wu, *ACS Catal.* **2014**, *4*, 2959-2968.

[42] T. Toyao, M. Saito, Y. Horiuchi, M. Matsuoka, *Catal. Sci. Technol.* **2014**, *4*, 625-628.

Table of Contents